Water Air Soil Pollut (2015) 226: 155
DOI 10.1007/s11270-015-2421-7

Intensify Removal of Nitrobenzene from Aqueous Solution Using Nano-Zero Valent Iron/Granular Activated Carbon Composite as Fenton-Like Catalyst

Sihai Hu · Hairui Yao · Kaifeng Wang · Cong Lu · Yaoguo Wu

Received: 5 November 2014 / Accepted: 10 April 2015 / Published online: 24 April 2015

Abstract To obtain a good catalytic effect of removing refractory organics from water by Fenton process, granular activated carbon (GAC) supported nano-zero valent iron (nZVI) composite (nZVI/GAC) was prepared by adsorption–reduction method, and characterized by scanning electron microscopy (SEM), X-ray diffraction (XRD), X-ray photoelectron spectroscopy (XPS), and energy-dispersive X-ray spectroscopy (EDS). The catalytic degradation activity of the composite was evaluated to remove nitrobenzene (NB) pollutant via a heterogeneous Fenton-like system, and the initial pH value, nZVI/GAC dosage, and H_2O_2 concentration influencing on NB removal were also investigated at room temperature. Experimental results showed that nZVI particle was uniformly dispersed over GAC matrix, and average particle size was 40–100 nm without agglomeration. The nZVI/GAC composite was very efficient in removing NB with average percentage of more than 85 %. However, the removal rate of Fenton-like reaction was highly affected by pH value, H_2O_2 concentration, and nZVI/GAC dosage. The optimal reaction conditions were pH 4.0, 40 mg/L NB, 5.0 mmol/L H_2O_2, and 0.4 g/L nZVI/GAC in this study. Stability and repeatability tests as well as mechanism analysis illustrated that GAC improved catalytic action via enhancing nZVI dispersion and accelerating Fe(III)/Fe(II) cycle attributing to internal iron–carbon microelectrolysis in nZVI/GAC composite. Iron utilization efficiency, which played an important role in NB degradation by Fenton-like greatly increased resulting in dissolved iron <0.6 mg/L. This phenomenon strongly implied that the nZVI/GAC Fenton-like process was not only a practical combination of adsorption and Fenton oxidation but also some synergetic effects existing in such an nZVI/GAC composite.

Keywords Fenton-like · nZVI/GAC composite · Nitrobenzene (NB) · Internal iron–carbon micro-electrolysis · Synergetic effects

S. Hu · H. Yao · K. Wang · C. Lu · Y. Wu (✉)
Key Laboratory of Space Applied Physics and Chemistry, Ministry of Education, Department of Chemistry, School of Science, Northwestern Polytechnical University, Xi'an 710072, People's Republic of China
e-mail: wuygal@163.com

S. Hu (✉) · H. Yao · K. Wang · C. Lu · Y. Wu
School of Science, Northwestern Polytechnical University, Youyi Road 127#,, Xi'an 710072, People's Republic of China
e-mail: hsh18621@163.com

1 Introduction

Nitrobenzene (NB) is an important chemical material of synthetic fuels, detergents, rubber, explosives, and other products, in which large amounts of waste containing NB are discharged into ecological environments (Haigler and Spain 1991; Mu et al. 2009). As an aromatic compound with stable chemical structure and high toxicity, NB is hard to be biodegraded and easily accumulated in environment, which is a potential risk to human beings and organisms (Mu et al. 2009; Wu et al. 2013a). For this reason, NB is listed as a priority control pollutant by the US EPA and other countries. In

China, the NB concentrations of industrial wastewater discharge (GB8978-1996) and surface water environmental quality standard (GB3838-2002) are <2.0 and 0.017 mg/L, respectively.

Among various physical, chemical, biological, and their combined technologies (Majumder and Gupta 2003; Wang et al. 2011; Zhang et al. 2014; Liang et al. 2014), advanced oxidation technologies (AOPs) are widely reported to be effective, reliable, and cost efficient for removing NB from water (Andreozzi et al. 1999; Ghatak 2014). As one of the important AOPs, Fenton has a good prospect on environmental protection to treat toxic and bio-refractory wastewater. The Fenton reaction describes the activation of hydrogen peroxide (H_2O_2) by ferrous ions (Fe(II)) to generate hydroxyl radicals (·OH) via a complex reaction sequence (Eqs. (1) and (2)) (Oturan and Aaron 2014; Shi et al. 2014).

$$\mathrm{Fe(II)} + \mathrm{H_2O_2} \rightarrow \mathrm{Fe(III)} + \cdot\mathrm{OH} + \mathrm{OH^-} \left(k = 63\text{–}76\ \mathrm{M^{-1}s^{-1}}\right) \quad (1)$$

$$\mathrm{Fe(III)} + \mathrm{H_2O_2} \rightarrow \mathrm{Fe(II)} + \cdot\mathrm{O_2H} + \mathrm{H^+} \left(k = 0.001\text{–}0.01\ \mathrm{M^{-1}s^{-1}}\right) \quad (2)$$

Fenton can be used either heterogeneous or homogeneous, and although the heterogeneous Fenton has great advantages in reducing iron loss, improving H_2O_2 efficiency, and decreasing iron sludge generation compared with homogeneous Fenton (Pignatello et al. 2006), there are still some obstacles in practical applications. For instance, Fe(II) is difficult to regenerate promptly, and the utilization efficiency is not high. Hence, the efficiency of Fenton oxidative degradation of NB is necessarily inefficient resulting in iron dosage large and difficult to control in practical applications (Singh et al. 2014; Shi et al. 2014).

Nano-zero valent iron (Fe^0, nZVI) has large specific surface area and high reactivity, and so the use of Fe^0 corrosion to provide Fe(II) for Fenton reaction has arisen wide attention (Nurmi et al. 2005). Under acidic conditions, Fe^0 can be corroded to generate Fe(II) and hydrogen (H_2) in situ, and in the presence of H_2O_2, Fenton reaction can take place as Fe(II) catalyses H_2O_2 to generate ·OH, and in the process, Fe(II) was oxidized to Fe(III) simultaneously. Then, Fe(III) can react with Fe^0 to form Fe(II) in the surface of nZVI, making the regeneration of Fe(II), and the reaction formulas are as follows (Hung et al. 2000; Segura et al. 2013):

$$\mathrm{Fe^0} + 2\mathrm{H^+} \rightarrow \mathrm{Fe(II)} + \mathrm{H_2} \quad (3)$$

$$\mathrm{Fe(II)} + \mathrm{H_2O_2} \rightarrow \mathrm{Fe(III)} + \cdot\mathrm{OH} + \mathrm{OH^-} \quad (4)$$

$$\mathrm{Fe^0} + 2\,\mathrm{Fe(III)} \rightarrow 3\,\mathrm{Fe(II)} \quad (5)$$

Therefore, as shown in Eqs. (3), (4), and (5), the utilization efficiency of iron will be greatly improved when nZVI is the source of iron because Fe(II) can be regenerated rapidly on the nZVI particle surface via nZVI reaction with Fe(III) produced during H_2O_2 decomposition. As a result, the actual catalytic effect of Fenton is not only enhanced but also easy to avoid the problem of excessive addition in real application (Bokare and Choi 2014). However, it is easy to find out that the catalytic effect is closely related to the nature of nZVI, which has been confirmed by many researches (Zhang et al. 2013a; Singh et al. 2014; Shi et al. 2014). The particle size of nZVI is small, so nZVI is easily agglomerated and oxidized by oxidative species in ambient conditions, leading to its deactivation rapidly (Zhang et al. 2013a, b; Wu et al. 2014; Busch et al. 2014). The deactivation of nZVI will reduce Fe(II) production efficiency via corrosion and limit electrons transfer between Fe^0 and Fe(III), which will hinder the circulations of Fe(II). Correspondingly, the efficiency of Fenton degradation NB will be severely affected as the catalytic activity of Fe(II) to H_2O_2 decreases.

Numerous studies have shown that nZVI immobilized on special supported materials may increase its dispersion, stability, and reactivity (Zhang et al. 2013a, b; Busch et al. 2014; Messele et al. 2015; Huang et al. 2014; Kerkez et al. 2014). Activated carbon (AC), as a cheap adsorbent used widely in water treatment, has abundant pores, various surface functional groups, and good hydraulic mechanical properties. Therefore, AC is an ideal carrier material of nZVI considering from the economy and effectiveness in water treatment (Pérez et al. 1997; Su et al. 2013; Subbaramaiah et al. 2014). Several studies also have concluded that AC is able to absorb NB and dissolved iron directly in water solution (Figueiredo et al. 1999; Kato et al. 2008; Chen et al. 2009a; Jadhav and

Srivastava 2013). Moreover, AC is found to act as catalysis of H_2O_2 decomposition to enhance ·OH yields (Pereira et al. 2010; Bach and Semiat 2011; Tan et al. 2013). Thus, the contact probability of ·OH and NB may be enhanced to increase Fenton oxidation effect. More importantly, recent studies have implied that iron–carbon corrosion galvanic effect can be formed between AC and iron (Dou et al. 2010; Mackenzie et al. 2012; Zhou et al. 2013; Wu et al. 2013b). This iron–carbon microelectrolysis is possible to significantly improve the electrons' transmission efficiency between Fe^0 and Fe(III), so Fe(II) regeneration will be enhanced to promote the recycle of iron. In addition, nZVI supported on AC is likely to decrease surface energy of nZVI, which can greatly improve its resistance to oxidation. Accordingly, nZVI supported on AC is likely to have a synergistic effect in such a composite system since Fe(II) regeneration will be more prompt and efficient. As a result, both the production rate and utilization efficiency of active ·OH will be strengthened. Ultimately, the effect of Fenton to remove organic pollutants will be intensified, and iron dosage will be reduced as well as dissolved iron concentration of wastewater solution after treatment.

In view of the above analysis, nZVI supported on granular activated carbon (GAC) (nZVI/GAC) composite was synthesized and characterized, then the effect of heterogeneous Fenton-like using nZVI/GAC as catalyst to remove NB was explored, and the influencing factors of pH, H_2O_2, and nZVI/GAC dosage on NB removal were evaluated, aiming to obtain a cost-effective Fenton-like method to remove refractory organics.

2 Materials and Methods

2.1 Materials Preparation

Nut shell-derived granular activated carbon (GAC) obtained from Gongyi Tongxin Water Treatment Material Co., Ltd (China) was used as the support of nZVI, and the particle size of GAC was 50 mesh (<0.3 mm). In order to avoid the influence of carbon black and other impurities, the GAC was washed by deionized water (R>18 MΩ) for 4 h and soaked in 1 M HNO_3 for 24 h followed by repeated rinsing with deionized water, and then placed in an vacuum drying oven at 105 °C until dry (Wang et al. 2014). Deionized water was used to prepare all reagents. An NB stock solution was prepared by dissolving 0.4 g NB in 1 L of deionized water, and the working solutions with designed concentrations of the experiment were prepared by diluting the stock solution.

2.2 Preparation and Characterization of nZVI/GAC Composite

The nZVI/GAC composite was prepared with reference to Wang et al. (2010) and Kim et al. (2013), and some improvements were made in the preparation. Briefly, 1 g of $FeSO_4{\cdot}7H_2O$ and 5 g of GAC were mixed in 200 mL of degassed deionized water. The pH of the solution was adjusted to 4.0 with 1 M HNO_3. The mixture was treated with ultrasound for 15 min, and then stirred vigorously at ambient temperature for over 12 h to achieve GAC adsorption of Fe(II) saturated. The slurry was rinsed five times using a mixture of ethanol and deionized water (1:1 v/v). To ensure efficient reduction of Fe(II), 50 mL of 1 M $NaBH_4$ solution was added at 30 drops/min while being stirred. The reduction reaction is as follows (Xiao et al. 2014):

$$\mathrm{Fe(II)} + 2\mathrm{BH_4^-} + 6\mathrm{H_2O} \rightarrow \mathrm{Fe^0} + 2\mathrm{B(OH)_3} + 7\mathrm{H_2}\uparrow \quad (6)$$

After sufficient reduction, the black solids were separated from the solution using a vacuum filtration flask (0.45 μm microporous membrane filter) and washed several times with degassed deionized water to remove residual sulfate. Then, the black solids were vacuum-dried at 60 °C and stored in a N_2-purged brown desiccator (Gu et al. 2005). Unsupported nZVI particles were also prepared in a similar way without GAC, and in all synthesis, high purity N_2 was bubbled into solution during the entire process to maintain an inert atmosphere.

Scanning electron microscopy (SEM; VEGA 3 LMH, TESCAN, Czekh) was used to view the surface characteristics and morphology of nZVI/GAC composite, and energy-dispersive X-ray spectra (EDS) were obtained using Oxford INCA X-ACT equipment in SEM. The element characteristics of the nZVI/GAC composite were obtained using X-ray photoelectron spectroscopy (XPS; Axis Ultra DLD, Kratos, UK) with Al K_α radiation. Core level spectra for C 1s, O 1s, and Fe 2p were taken at high resolution and analyzed for chemical state information. Bruker powder diffractmeter (Model D8, Germany) with Cu $K_{\alpha1}$ radiation (k=

0.154 nm) was employed to characterize crystal of the nZVI/GAC samples, and the X-ray diffraction patterns were recorded in the range of 2θ=10–80 °. The instrument was operated at 40 kV and 30 mA, and the spectra were recorded at a scanning speed of 1 °/min (2θ) and a step of 0.01 nm.

2.3 Batch Experiments

The stock solution of NB was diluted into 40 mg/L as model wastewater samples, and then 200 mL was placed in a 250-mL flask and adjusted pH values with 1 mol/L H_2SO_4. The dosages of nZVI/GAC and H_2O_2 solution were added according to the designed Fe(II) and H_2O_2 molar ratio. The flask was placed on a magnetic stirrer thermostatic mixing at 300 rpm and sampled regularly, and the NB concentrations were determined using high-performance liquid chromatography (HPLC) equipped with a Waters symmetry C-18 column (150 mm× 4.6 mm i.d., 5 μm). The mobile phase was the mixture of methanol and 5 mM H_3PO_4 in the ratio of 3:2 (*v*/*v*). The flow rate was set at 1 mL/min, and the detection wavelength was set to 267.5 nm. The ultraviolet absorption spectra were recorded with a Shimadzu spectrophotometer (UV-2550, Japan) and using quartz cells of 10 mm optical path. To prepare iron samples for SEM and X-ray diffraction (XRD) analysis, the bulk solution in the flask was discarded at a designated reaction time. The nZVI/GAC particles that remained in the flask were then washed three times with deionized water and dried in vacuum drying oven. All the prepared samples were taken for analysis immediately. Pure adsorption runs were also performed in order to assess the contribution of GAC adsorption to NB removal, and the experiments were carried out in the same conditions as described above without H_2O_2 addition. GAC adsorption and Fenton-like experiments were conducted in triplicate, and analyses showed that relative errors were lower than ±5 %.

3 Results and Discussion

3.1 Characterization of nZVI/GAC Composite

Studies have shown that GAC has the uniform porous and abundance functional nature, and these pores and functions provide a good possibility for nZVI particles to be trapped inside of them (Pérez et al. 1997; Su et al. 2013; Subbaramaiah et al. 2014). Figure 1a implied that, in the absence of GAC, iron particles were found to agglomerate more rapidly to chain due to the large surface energy of nanoparticles. In comparison, as is revealed in Fig. 1b, the iron particles were well dispersed on the surface or pores of GAC carrier without any aggregation, and the particles size supported on GAC were 40–100 nm on average by comparison with a standard ruler. The SEM images (Fig. 1a, b) confirmed the presence of both iron and GAC in the composite, and the iron particles were uniformly dispersed over GAC matrix with a nanometer scale. Therefore, the composite morphology studied by SEM clearly reveals that iron particles are able to distribute over GAC with nanoscale. Meanwhile, the results also demonstrate that GAC is a good carrier of nanoiron and has well potential capability to prevent nanoiron particles from aggregating together to chains.

Figure 1c is the XRD pattern of nZVI/GAC composite; it was obvious that the characteristic peaks were at 2θ=24.8, 38.5, and 44.9 °. The broad peak at 2θ=24.8 ° (C 002) confirmed the presence of GAC in the composite (Zhang et al. 2013a, b). The marked XRD characteristic peak of zero valent iron was about 45 ° (2θ), which had been evidenced by some investigations (Zhang et al. 2006; Singh et al. 2014), so the diffraction peak at 44.9 ° observed in the composite samples confirms that the formation of iron was zero valence (shown in Fig. 1c). Hence, from the results of SEM and XRD, we can conclude that the iron particles in the composition were nZVI. The crystalline size of the nZVI in the composite was calculated using the Debye–Scherer formula and found to be about 50 nm, and these results were in approximation with SEM analysis. Moreover, in the spectrum of XRD, strong diffraction peaks of Fe_3O_4 (2θ=35.46, 43.12, 53.50, 56.98, and 62.64 °) were not found, and it was clear that the oxidation of nZVI did not occur severely after supported on GAC, and thus, it was easy to infer that the nZVI/GAC composite had some antioxidant ability.

The iron states presented on GAC were also evaluated by XPS (Fig. 1d). For a better observation of the iron states, a narrow scan from 740 to 700 eV was conducted (Fig. 1e). From the XPS spectra, significant differences were observed for GAC and the nZVI/GAC composite. On the surface, iron seemed to be of three states: One was zero valent state at 706.8 eV, which was for zero valent iron (ZVI, Fe^0), and the other two were oxidation states at 710 and 725 eV. The one at 725 eV was for iron

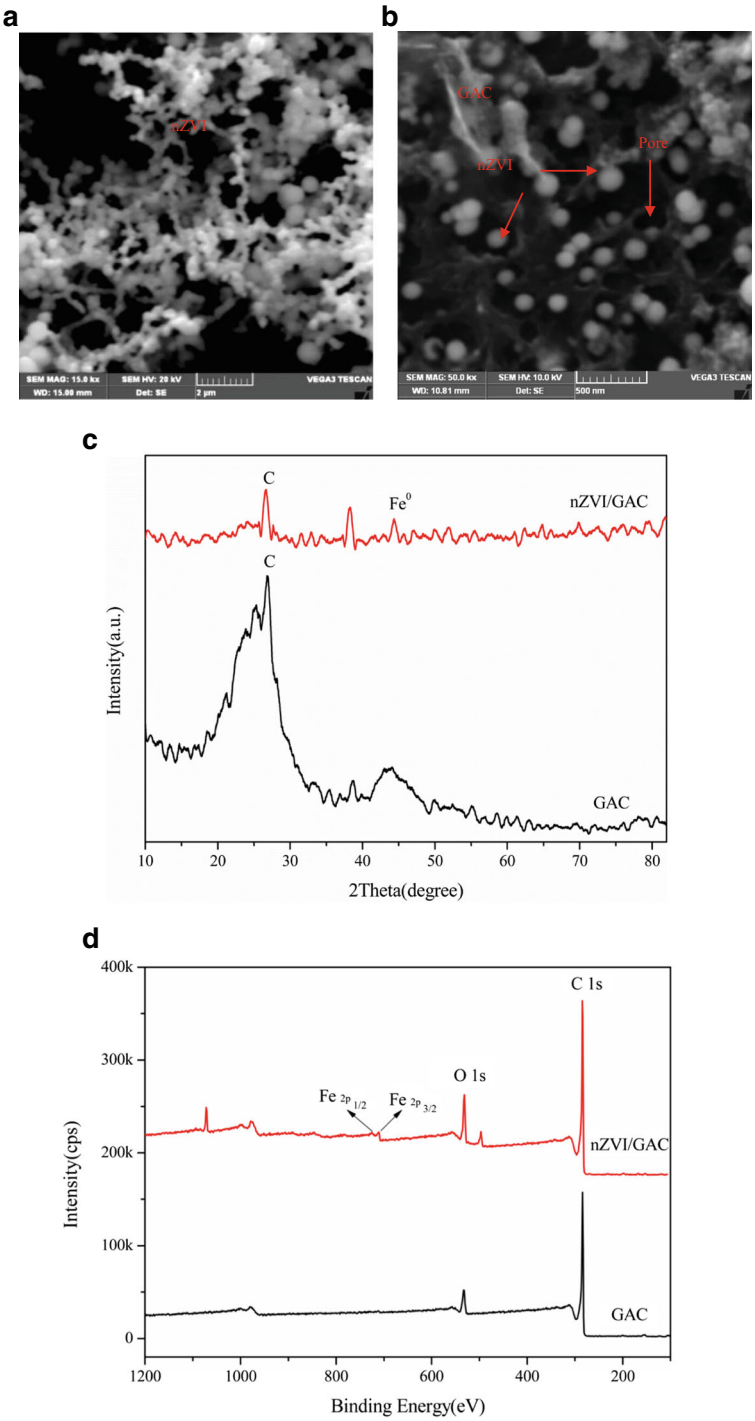

Fig. 1 SEM images (**a**, **b**), XRD (**c**), XPS (**d**, **e**), and EDS (**f**) of the nZVI/GAC composite

in Fe_3O_4, and the other at 710 eV was at lower oxidation state for FeO (Kim et al. 2013). Therefore, the XPS results clearly indicated that the nZVI particles dispersed on GAC were Fe^0. These findings were in good agreement with those obtained from other technical characterizations of SEM and XRD analysis, which also suggested the formation of small iron particles dispersed over GAC. The content of nZVI in the composite

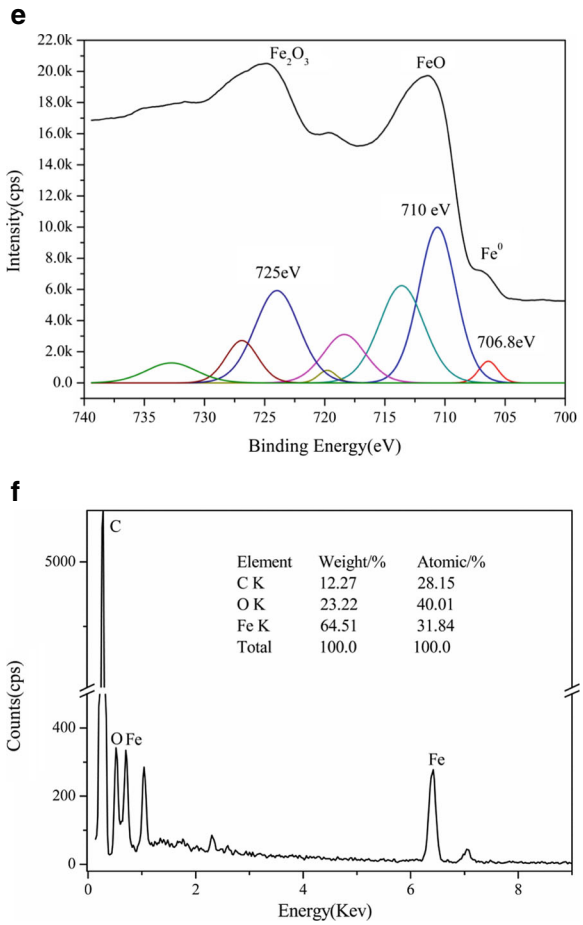

Fig. 1 (continued)

surface determined by EDS was exhibited in Fig. 1f. The iron content is high to 64.51 % in the surface of nZVI/GAC composite, and the total load iron was 64.3 μmol/g obtained by the composite dissolved in acid solution, further suggesting that nZVI has been supported on GAC successfully.

Overall, Fig. 1 illustrates that nZVI particles disperse uniformly well with average diameters of 40–100 nm on the surface or inside pores of the GAC, and the nZVI content reaches to 64.51 % in the surface of nZVI/GAC composite. This can be explained that, when nZVI particles were adsorbed on the surface or pores of GAC, nZVI particles did not agglomerate together because of the increase in electrostatic repulsion and steric effect between iron atoms. Eventually, the magnetic attraction decreased; meanwhile, soft reunite, surface electronic effects, and close effect caused by small size effect of nano-particles were overcome well, and therefore, the dispersion of nZVI was greatly improved.

3.2 Fenton Degradation of Nitrobenzene in the Presence of nZVI/GAC Composite

As we know, carbon materials are, moreover, good adsorbent and catalyst in different reactions (Carrasco-Marín et al. 1998; Moreno-Castilla et al. 1998; Thankappan et al. 2015). For this reason, the catalytic behaviors of both GAC and nZVI/GAC catalysts were evaluated in the presence and absence of H_2O_2, and NB removing from aqueous solution was used to investigate their catalytic activity. In the experiments, the quantity of bare GAC was equal to the amount in nZVI/GAC composite calculated by nZVI loading amount. The results on different experimental conditions are depicted in Fig. 2. As is shown in the traces, the removal rates of NB were measured to be 10.0 % for H_2O_2, 17.4 % for GAC, 32.7 % for GAC with H_2O_2, 36.5 % for

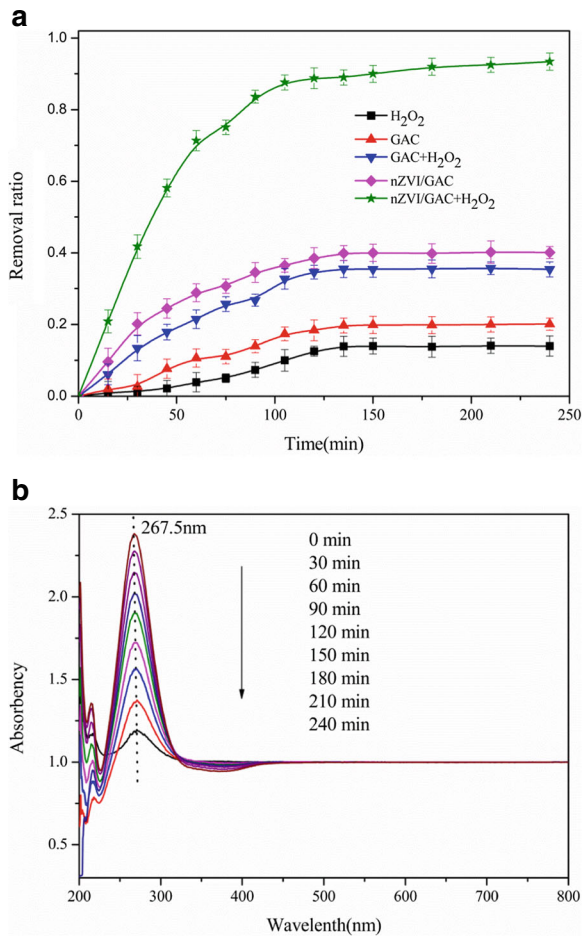

Fig. 2 Removal ratio changes of NB (40 mg/L) under different conditions (**a**), and UV–vis spectra of NB decomposition. Experimental conditions: 0.2 g/L nZVI/GAC, pH 4.0 (**b**), and T=25 °C

nZVI/GAC composite, and 87.5 % for H_2O_2 with nZVI/GAC composite after 100 min, respectively.

There was only a little removal of NB observed in the presence of bare H_2O_2 or GAC. For example, GAC could only remove 32.7 % of NB in the presence of H_2O_2. In addition, about 36.5 % of NB was removed for nZVI/GAC in the absence of H_2O_2 system, which indicated that GAC and nZVI/GAC were positive catalyst functions for the elimination of NB to some extent. As a contrast, when both nZVI/GAC and H_2O_2 existed in the aqueous solution, almost 100 % of NB was removed at 100 min. These results suggested that GAC had the absorption for NB and a catalytic effect to H_2O_2, and nZVI/GAC had a reduction ability of NB leading to NB concentration decrease, but the removal ratio was low. By comparison, when nZVI/GAC acted as an efficient catalyst for H_2O_2, the removal ratio increased greatly from <40 % to more than 85 % which was obviously higher than the sum of GAC and nZVI/GAC single (17.4 and 36.5 %). This phenomenon strongly illustrated that the process of NB removal was not only an excellent combination of adsorption by GAC and Fenton oxidation by nZVI but also some synergetic effects existing in such a composite.

It was clear that minor NB was adsorbed onto the surface of GAC leading to low NB removal rate because of limited adsorption sites. This result also suggested that extremely low-quantity absorption of NB existed in the solution, and the removal was dominantly attributed to the Fenton effect instead of adsorption. The nZVI/GAC acted as an efficient catalyst for H_2O_2 activation to remove NB. Thus, the most efficient removals for NB were achieved by the nZVI/GAC Fenton-like system. It could be easy to infer that the oxidation by Fenton and the adsorption by GAC played their mutual promotion roles in the NB removal process. As a support material, GAC can disperse nZVI and prevent nZVI from aggregation. Consequently, considerable reaction activity of Fenton-like catalyzed by nZVI/GAC composite was obtained, and moreover, the composite material was able to exploit the mutual adsorption of GAC for NB resulting in the total NB concentration decrease.

The absorption spectra of reaction solution were scanned in the range of 200–800 nm, as given in Fig. 2b. Regarding the UV-vis spectra, it was characterized by one band in ultraviolet region located at 267.5 nm, which was the characteristic peak of NB (Nichela et al. 2008), and the peak intensity decreased with increase in reaction time. The UV band absorption is attributed to the $\pi \rightarrow \pi$ transition of aromatic rings in NB molecule. Obviously, the band located at 267.5 nm decreased rapidly following reaction time and tended to miss after 120 min of reaction; however, the appearance of new adsorption bands in the visible region were not observed. This reflected that the removal of NB was practically complete (Nguyen et al. 2011).

3.3 Effects of Nitrobenzene Removal by nZVI/GAC Composite Fenton-Like

Since pH values, nZVI/GAC dosages, and H_2O_2 concentrations are the most important reaction parameters influencing on NB removal in the nZVI/GAC Fenton-like system. Therefore, typical experiments were carried out individually to check the extent of NB removing from aqueous solutions.

3.3.1 Effect of nZVI-GAC Dosages

Removal efficiency using Fenton-like process for NB wastewater treatment is influenced by the concentration of Fe(II), which catalyzes H_2O_2 decomposition to active ·OH to oxidative degradation organics (Ganzenko et al. 2014; Hung et al. 2000). Generally, an extreme dosage of iron can contribute to significant improvement in the removal efficiency but an obvious increase in dissolved iron and iron sludge simultaneous (Segura et al. 2013). Therefore, excessive iron salt dosage tends to need a further treatment for the effluent before its discharge into the receiving water body (Gogate and Pandit 2004). Figure 3 shows the effect of nZVI/GAC dosage change

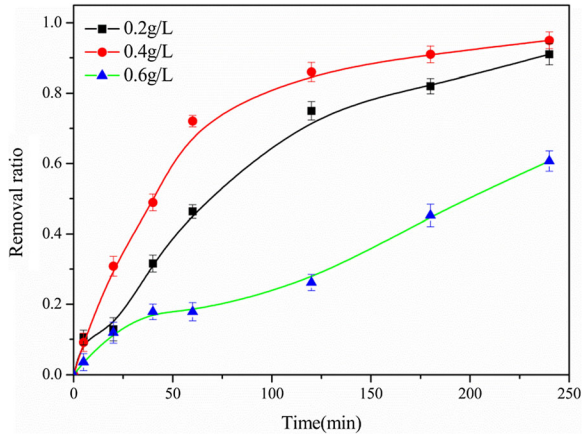

Fig. 3 Effect of different nZVI/GAC dosages on Fenton-like removal process of NB wastewater. Experimental conditions: pH=3.0, 2.5 mmol/L H_2O_2, and T=25 °C

on NB removal, and the impact was investigated in the range of 0.2–0.6 g/L nZVI/GAC catalyst. As is shown in Fig. 3, the degradation efficiency increased with the catalyst dosage up to 0.4 g/L, but then it slightly decreased upon further addition of the catalyst. The fairly well-removal efficiency was achieved at the amount of catalyst dosage 0.4 g/L under the experimental conditions.

It has been reported that an excess of ferrous ions will consume ·OH; for this reason, in this experiment, no improvements have been attained when there was an increase on nZVI/GAC dosage to 0.6 g/L at H_2O_2 concentration 2.5 mmol/L (see inset in Fig. 3). The same phenomenon has been reported by Liao et al. (2009). The inhibition effect of iron species is considered as the reason for the decrease because the scavenging of ·OH or other radicals will occur when presenting excessive metal species, which can be expressed by the following equations (Liao et al. 2009; Romero et al. 2009; Ramirez et al. 2007; Lam et al. 2005).

$$\mathrm{Fe(II)} + \cdot\mathrm{OH} \rightarrow \mathrm{Fe(III)} + \mathrm{OH^-} \quad (7)$$

$$\mathrm{Fe(II)} + \cdot\mathrm{OOH} \rightarrow \mathrm{Fe(III)} + \mathrm{OOH^-} \quad (8)$$

3.3.2 Effect of H_2O_2 Concentrations

Figure 4 shows the effect of H_2O_2 dosage on NB degradation in the range of 2.5–10.0 mmol/L. The removal efficiency of NB was raised obviously when H_2O_2 concentration increased from 2.5 to 5.0 mmol/L. The enhancement of the removal rate by addition of H_2O_2 is due to an increase in ·OH yield. However, it should be pointed out that the degradation rate of NB decreased when the concentration of H_2O_2 exceeded 5.0 mmol/L. This can be explained by the scavenging of ·OH at a higher H_2O_2 dosage, leading to a decline of ·OH generation in solution (Eqs. (8) and (9)) (Parra et al. 2004; Chen et al. 2009a, b).

$$\mathrm{H_2O_2} + \cdot\mathrm{OH} \rightarrow \mathrm{H_2O} + \cdot\mathrm{OOH} \quad (9)$$

$$\cdot\mathrm{OOH} + \cdot\mathrm{OH} \rightarrow \mathrm{H_2O} + \mathrm{O_2} \quad (10)$$

3.3.3 Effect of Initial pH Values

To assess the effect of initial pH on the catalytic oxidation of NB, a series of experiments were performed where the solution pH was adjusted to 3.0, 4.0, and 5.0. The obtained results (Fig. 5) showed that, for both samples used, the NB removal ratio increased when the pH increased from 3.0 to 4.0, but decreased when the pH increased to 5.0. These observations are consistent with previously reported results (Yao et al. 2013; Ramirez et al. 2007; Thankappan et al. 2015). Obviously, the nZVI/GAC catalyst has been active in studying pH between 3.0 and 5.0. For example, at pH 3.0, 4.0, and 5.0, about 81.0, 91.6, and 86.0 % of NB were degraded by the nZVI/GAC composite catalyst, respectively, after 120 min of reaction.

Figure 5 also implied that the best result of NB degradation for the composite catalyst was at pH 4.0,

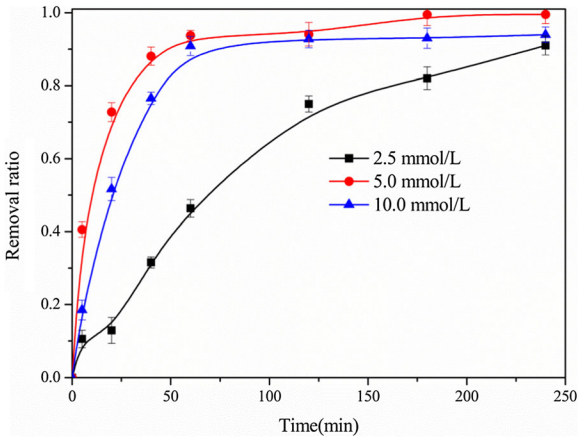

Fig. 4 Effect of H_2O_2 concentration on the degradation of NB. Experimental conditions: 40 mg/L NB, 0.4 g/L nZVI/GAC, pH 3.0, and T=25 °C

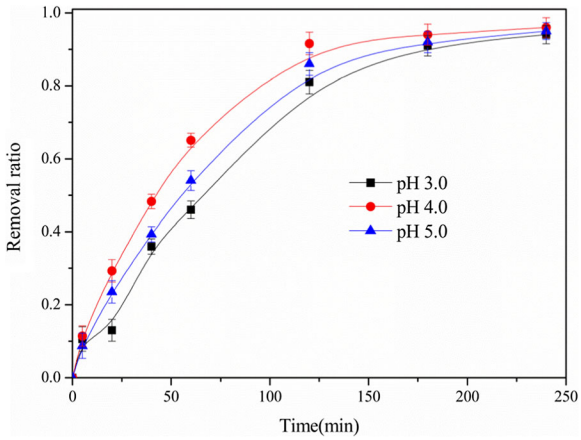

Fig. 5 pH effect on the degradation of NB solution using nZVI/GAC. Experimental conditions: 40 mg/L NB, 5.0 mmol/L H_2O_2, 0.4 g/L nZVI/GAC, and T=25 °C

and its catalytic activity was still kept up until pH was over 5.0. This conclusion was remarkably well supported by the result that the removal ratio of NB was still 86.0 % at pH 5.0. Moreover, the final pH values of the solution after reaction were 6.4, 6.7, and 6.8 for the initial pH of 3.0, 4.0, and 5.0. These are important advantages because it is well known that one major drawback of the homogeneous Fenton process is pH range narrow (pH<3.0) (Pignatello et al. 2006), and such a narrow pH range is unfavorable in practice due to the costs of acidification during processing and neutralization after nZVI Fenton-like treatment. For these reasons, further experiments will be carried out at pH over 5.0 using the most promising catalyst of nZVI/GAC composite for refractory organic degradation.

3.4 Stability and Repeatability of nZVI/GAC Composite

The research conducted by Singh et al. (2014) has indicated that NB removal efficiency decreased sharply in the following six cycles using Fe^0 as Fenton-like catalyst, and this can be explained as follows. First, a small amount of oxygen was introduced into the reaction system during repeated process, leading to Fe^0 oxidation and reaction sites loss during continuous degradation. Second, iron corrosion in each Fenton reaction could induce the incorporated iron particles partially dissolved into the solution (Nguyen et al. 2011). Hence, in practice, to use a heterogeneous catalyst in Fenton-like oxidation, it is crucial to evaluate the stability and repeatability of catalyst. To investigate the stability of nZVI/GAC composite, oxidation resistance in air condition was investigated via iron content change in the composite recorded by EDS, and the results are shown in Fig. 6a. As is seen in Fig. 6a, the content of iron both in bare nZVI and nZVI/GAC composite decreased with stored time prolong in nature air condition (25 °C) because of the oxidization, but the rate of decrease was significantly changed from 0.344 for nZVI to 0.159 for nZVI/GAC composite, which reduced by half nearly. Consequently, it is easy to see from the results that the stability of nZVI in air was markedly improved after being carried on GAC, suggesting that the nZVI/GAC composite has some oxidation resistance.

The recycle efficiency of nZVI/GAC composite was explored under H_2O_2 system. The separation of

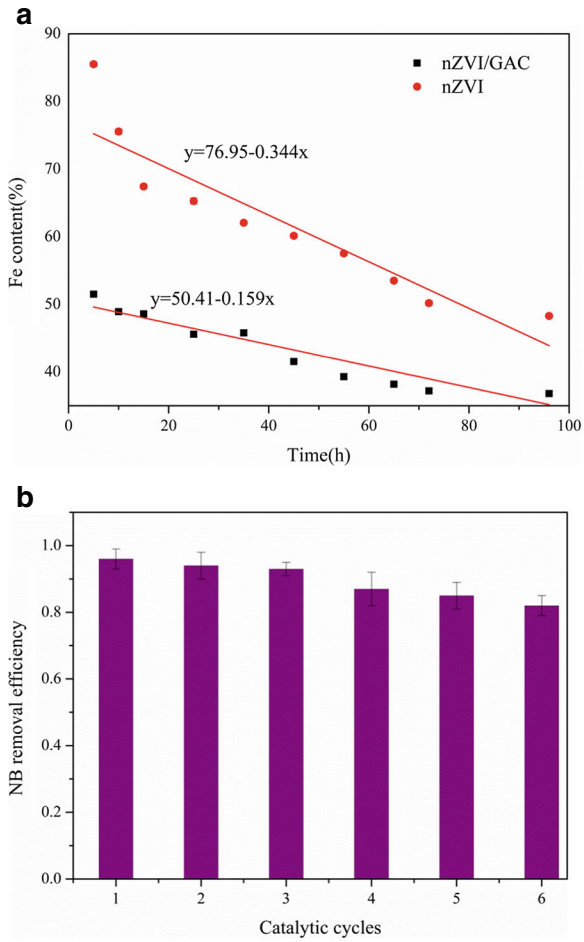

Fig. 6 The change of iron content with storage time in the air (**a**) and recycle efficiency of nZVI/GAC composite (**b**)

nZVI/GAC composite was quick and easy due to low agglomeration. However, Singh et al. (2014) reported that separation of nZVI particles was slow and complicated, and the efficiency of nZVI was reduced about 70 % after six catalytic cycles. Hence, the stability of nZVI/GAC was further investigated by means of recycling experiments with the same sample recovered by filtration after each cycle. A set of nZVI/GAC was used as the catalyst according to the process described previously at the conditions of 40 mg/L NB, 0.4 g/L nZVI/GAC, 5.0 mmol/L H_2O_2, and pH 4.0. After each cycle, the composite was taken out and rinsed with deionized water to remove the residual H_2O_2 and then dried at room temperature. This process was repeated six times. As is shown in Fig. 6b, only a little amount of removal ratio (<3.0 %) decreased for the catalytic reaction in each recycling experiment, and the catalytic

activity decreased only 14.0 % after six runs. It is obvious that the Fenton-like catalyst of nZVI/GAC composite is relatively stable for NB removal, which is consistent with the above results. Hereby, the nZVI/GAC composite is an antioxidative and reusable heterogeneous Fenton-like catalyst.

3.5 Intensify Mechanism of nZVI/GAC Composite Fenton-Like Degradation Nitrobenzene

Fenton oxidation reaction involves the application of ferrous ions to react with H_2O_2 to generate ·OH with a strong oxidizing ability to degrade organic pollutants. However, the mechanism of Fenton reaction is still under intense and controversial discussion. Generation of ·OH by the dark reaction of H_2O_2 with ferrous salt has been the subject of numerous studies during the last decade (Chan and Chu 2003). The general mechanism is using Fenton reagents to produce ·OH, which is a number of cyclic reactions utilizing Fe(II) or Fe(III) ion as a catalyst to decompose H_2O_2. These catalytic activity ions are regenerated in their original state at the end of the cyclic reactions according to the above equations (Eqs. (3) and (4)) (Medien and Khalil 2010). The species of iron are very important to deduce the catalytic reaction mechanism. Accordingly, the composite catalyst after Fenton-like reaction was dried under vacuum oven and then tested by XPS. Meanwhile, the dissolved iron during the reaction was monitored under optimal condition with initial pH 4.0, 0.4 g/L nZVI/GAC, and 5.0 mmol/L H_2O_2. The results are presented in Fig. 7a and b. It can be seen from that the dissolved iron was below 0.6 mg/L in the Fenton-like process. This suggests that the iron leaching reaches very low level in the reaction, which is a crucial factor for the composite catalyst long-term use. After Fenton-like reaction, the Fe^0 spectrum almost decreased to miss, while Fe(III) content increased, which were illustrated by the XPS spectra (Fig. 7b) (Chan and Chu 2003). Results presented by Mackenzie et al. (2012) have indicated that AC can reduce the effluent by-product concentration; in addition, the research of Dou et al. (2010) has shown that Fe^0 and carbon can form a micro-electrolysis, which can speed up the rate of reaction via enhancing ·OH formation. Our results are therefore in good agreement with these conclusions. The catalytic activity of the composite catalyst to Fenton-like reaction seems to be more directly related with the special element and structural characteristics of the carrier GAC.

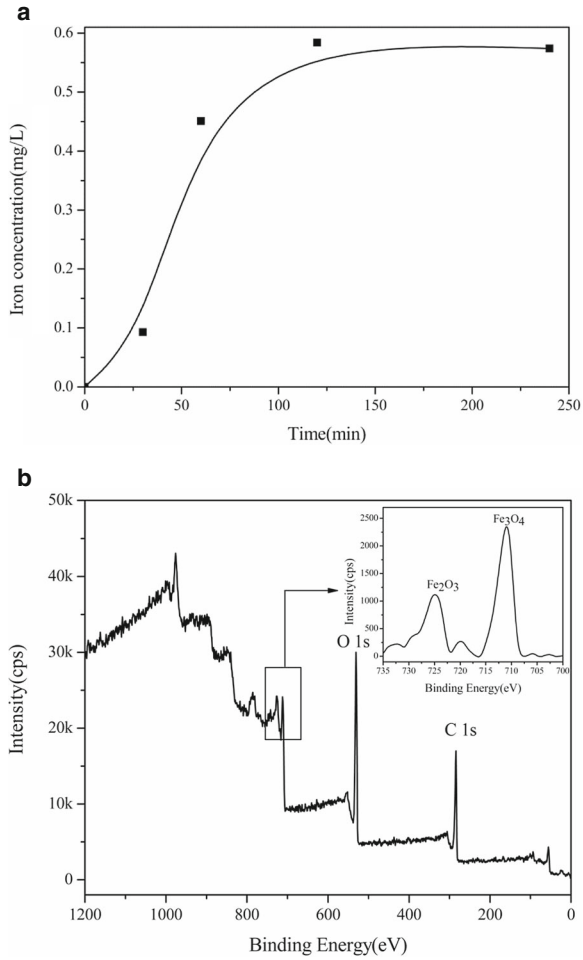

Fig. 7 Effect of Fe(II) production on Fenton-like removal of NB (**a**) and the XPS spectrum of nZVI/GAC after Fenton-like reaction. (**b**) Experimental conditions: 40 mg/L NB, 0.4 g/L nZVI/GAC, 5.0 mmol/L H_2O_2, pH 4.0, and T=25 °C

Based on the above analysis, we propose a mechanism of the nZVI/GAC composite to enhance the catalytic ability for NB removal. First, nZVI dispersed on GAC very well without agglomeration, and their contact surface with solution is increased to accelerate the conversion of Fe^0 to Fe(II), thereby promoting H_2O_2 decomposition to generate ·OH (Velo-Gala et al. 2014). In turn, Fe(II) is regenerated promptly in situ via Fe(III) reacting with Fe^0 in the surface or pores of nZVI/GAC composite. Iron and GAC can form a microgalvanic cell, and the efficiency of electron transfer is increased due to GAC as migration medium to promote the regeneration and circulation of Fe(II). In such case, the utilization efficiency of iron is improved and iron loss is reduced, and therefore, GAC accelerates the whole

Fe(III)/Fe(II) cycle and makes dissolved iron <0.6 mg/L (Fig. 7a), indicating that GAC plays an important role in NB degradation. Furthermore, the super oxide radical, which has much lower oxidation ability than OH, is not formed in this heterogeneous catalyst system because of the internal iron–carbon microelectrolysis to accelerate H_2O_2 decomposition, which is very different from the corresponding homogeneous Fenton system. This difference suggests that it is very efficient to use nZVI/GAC composite to increase the amount of OH generation in heterogeneous catalytic system, which results in the nZVI/GAC's higher catalytic ability. In addition, GAC has large surface area, abundance pores, and various functional groups, which can provide active sites for NB sorption benefiting NB degradation by OH effectively. Consequently, the enriched NB can be efficiently and rapidly removed by OH in a strong Fenton-like oxidation process. In general, NB was removed efficiently by the nZVI/GAC Fenton-like system in the synergetic effect of nZVI and GAC.

4 Conclusions

The involvement of GAC improved the dispersion of nZVI greatly and intensified the removal of NB from aqueous solution with less dissolved iron after Fenton-like reaction, as GAC in the composite performed as both a reactive support in iron-rich phase and a catalyst promoter on ·OH generation, and there were iron–carbon microelectrolysis effects to promote electrons transfer efficiency to enhance Fe(III)/Fe(II) regeneration and cycles. Mechanism analysis illustrated that the Fenton-like to remove NB catalyzed by nZVI/GAC composite was not only a perfect combination of adsorption by GAC and Fenton oxidation by nZVI but also some synergetic effects existing in such a composite. Therefore, the present study may not only pave a new avenue for designing efficient and cheap Fenton-like catalysts but also provide a preferable practical approach to treat refractory wastewater containing NB. This novel system represents an important insight on the development of new inexpensive and efficient chemical materials to environmental remediation processes, but the mechanism needs to be studied profoundly and the hydrogen produced during the nZVI/GAC Fenton-like reaction cannot be ignored as well.

Acknowledgments The authors gratefully acknowledge the financial support by the National Natural Science Foundation of China (Grant No. 40872164), fund for basic research from the Northwestern Polytechnical University (No. JCY20130145), and China geological survey project (12120114056201).

References

Andreozzi, R., Caprio, V., Insola, A., & Marotta, R. (1999). Advanced oxidation processes (AOP) for water purification and recovery. *Catalysis Today, 53*(1), 51–59.

Bach, A., & Semiat, R. (2011). The role of activated carbon as a catalyst in GAC/iron oxide/H_2O_2 oxidation process. *Desalination, 273*(1), 57–63.

Bokare, A. D., & Choi, W. Y. (2014). Review of iron-free Fenton-like systems for activating H_2O_2 in advanced oxidation processes. *Journal of Hazardous Material, 275*, 121–135.

Busch, J., Meißner, T., Potthoff, A., & Oswald, S. E. (2014). Transport of carbon colloid supported nanoscale zero-valent iron in saturated porous media. *Journal of Contaminant Hydrology, 164*, 25–34.

Carrasco-Marín, F., Mueden, A., & Moreno-Castilla, C. (1998). Surface-treated activated carbons as catalysts for the dehydration and dehydrogenation reactions of ethanol. *Journal of Physical Chemistry B, 102*, 9239–9244.

Chan, K. H., & Chu, W. (2003). The system design of atrazine oxidation by catalytic oxidation process through a kinetic approach. *Water Research, 37*(16), 3997–4003.

Chen, M., Cui, L., Li, C. H., & Diao, G. W. (2009a). Adsorption, desorption and condensation of nitrobenzene solution from active carbon: A comparison of two cyclodextrins and two surfactants. *Journal of Hazardous Materials, 162*(1), 23–28.

Chen, Q. Q., Wu, P. X., Li, Y. Y., Zhu, N. W., & Dang, Z. (2009b). Heterogeneous photo-Fenton photodegradation of reactive brilliant orange X-GN over iron-pillared montmorillonite under visible irradiation. *Journal of Hazardous Materials, 168*(2-3), 901–908.

Dou, X. M., Li, R., Zhao, B., & Liang, W. Y. (2010). Arsenate removal from water by zero-valent iron/activated carbon galvanic couples. *Journal of Hazardous Materials, 182*(1-3), 108–114.

Figueiredo, J. L., Pereira, M. F. R., Freitas, M. M. A., & Órfão, J. J. M. (1999). Modification of the surface chemistry of activated carbons. *Carbon, 37*(9), 1379–1389.

Ganzenko, O., Huguenot, D., van Hullebusch, E. D., Esposito, G., & Oturan, M. A. (2014). Electrochemical advanced oxidation and biological processes for wastewater treatment: A review of the combined approaches. *Environmental Science and Pollution Research, 21*(14), 8493–8524.

Ghatak, H. R. (2014). Advanced oxidation processes for the treatment of biorecalcitrant organics in wastewater. *Critical Reviews in Environmental Science and Technology, 44*(11), 1167–1219.

Gogate, P. R., & Pandit, A. B. (2004). A review of imperative technologies for wastewater treatment I: Oxidation technologies at ambient conditions. *Advances in Environmental Research, 8*(3-4), 501–551.

Gu, Z. M., Fang, J., & Deng, B. L. (2005). Preparation and evaluation of GAC-based iron containing adsorbents for arsenic removal. *Environmental Science and Technology, 39*(10), 3833–3843.

Haigler, B. E., & Spain, J. C. (1991). Biotransformation of nitrobenzene by bacteria containing toluene degradative pathways. *Applied and Environmental Microbiology, 57*(11), 3156–3162.

Huang, L. H., Zhou, S. J., Jin, F., Huang, J., & Bao, N. (2014). Characterization and mechanism analysis of activated carbon fiber felt-stabilized nanoscale zero-valent iron for the removal of Cr (VI) from aqueous solution. *Colloid and Surface A: Physicochemical and Engineering Aspects, 447*, 59–66.

Hung, H. M., Ling, F. H., & Hoffmann, M. R. (2000). Kinetics and mechanism of the enhanced reductive degradation of nitrobenzene by elemental iron in the presence of ultrasound. *Environmental Science & Technology, 34*(9), 1758–1763.

Jadhav, A. J., & Srivastava, V. C. (2013). Adsorbed solution theory based modeling of binary adsorption of nitrobenzene, aniline and phenol onto granulated activated carbon. *Chemical Engineering Journal, 229*, 450–459.

Kato, Y., Machida, M., & Tatsumoto, H. (2008). Inhibition of nitrobenzene adsorption by water cluster formation at acidic oxygen functional groups on activated carbon. *Journal of Colloid and Interface Science, 322*(2), 394–398.

Kerkez, D. V., Tomašević, D. D., Kozma, G., Bečelić-Tomin, M. R., Prica, M. D., Ronćević, S. D., Kukovecz, A., Dalmacija, B. D., & Kónya, Z. (2014). Three different clay-supported nanoscale zero-valent iron materials for industrial azo dye degradation: A comparative study. *Journal of Taiwan Institute of Chemical Engineers, 45*(5), 2451–2461.

Kim, S. A., Kamala-Kannan, S., Lee, K. J., Park, Y. J., Shea, P. J., Lee, W. H., Kim, H. M., & Oh, B. T. (2013). Removal of Pb(II) from aqueous solution by a zeolite–nanoscale zero-valent iron composite. *Chemical Engineering Journal, 217*, 54–60.

Lam, S. W., Chiang, K., Lim, T. M., Amal, R., & Low, G. K. C. (2005). The role of ferric ion in the photochemical and photocatalytic oxidation of resorcinol. *Journal of Catalysis, 234*(2), 292–299.

Liang, B., Cheng, H. Y., Van Nostrand, J. D., Ma, J. C., Yu, H., Kong, D. Y., Liu, W. Z., Ren, N. Q., Wu, L. Y., Wang, A. J., Lee, D. J., & Zhou, J. Z. (2014). Microbial community structure and function of nitrobenzene reduction biocathode in response to carbon source switchover. *Water Research, 54*, 137–148.

Liao, Q., Sun, J., & Gao, L. (2009). Degradation of phenol by heterogeneous Fenton reaction using multi-walled carbon nanotube supported Fe_2O_3 catalysts. *Colloids and Surfaces A: Physicochemical and Engineering Aspects, 345*(1-3), 95–100.

Mackenzie, K., Bleyl, S., Georgi, A., & Kopinke, F. D. (2012). Carbo-Iron-An Fe/AC composite-As alternative to nano-iron for groundwater treatment. *Water Research, 46*(12), 3817–3826.

Majumder, P. S., & Gupta, S. K. (2003). Hybrid reactor for priority pollutant nitrobenzene removal. *Water Research, 37*(18), 4331–4336.

Medien, H. A. A., & Khalil, S. M. E. (2010). Kinetics of the oxidative decolorization of some organic dyes utilizing Fenton-like reaction in water. *Journal of King Saud University-Science, 22*(3), 147–153.

Messele, S. A., Soares, O. S. G. P., Órfão, J. J. M., Bengoa, C., Stüber, F., Fortuny, A., Fabregat, A., & Font, J. (2015). Effect of activated carbon surface chemistry on the activity of ZVI/AC catalysts for Fenton-like oxidation of phenol. *Catalysis Today, 240*, 73–79.

Moreno-Castilla, C., Carrasco-Marin, F., Maldonado-Hodar, F. J., & Rivera-Utrilla, J. (1998). Effects of non-oxidant and oxidant acid treatments on the surface properties of an activated carbon with very low ash content. *Carbon, 36*(1-2), 145–151.

Mu, Y., Rozendal, R. A., Rabaey, K., & Keller, J. (2009). Nitrobenzene removal in bioelectrochemical systems. *Environmental Science & Technology, 43*(22), 8690–8695.

Nguyen, T. D., Phan, N. H., Do, M. H., & Ngo, K. T. (2011). Magnetic Fe_2MO_4 (M: Fe, Mn) activated carbons: Fabrication, characterization and heterogeneous Fenton oxidation of methyl orange. *Journal of Hazardous Materials, 185*(2-3), 653–661.

Nichela, D., Carlos, L., & Einschlag, F. G. (2008). Autocatalytic oxidation of nitrobenzene using hydrogen peroxide and Fe (III). *Applied Catalysis B: Environmental, 82*(1-2), 11–18.

Nurmi, J. T., Tratnyek, P. G., Sarathy, V., Baer, D. R., Amonette, J. E., Pecher, K., Wang, C. M., Linehan, J. C., Matson, D. W., Penn, R. L., & Driessen, M. D. (2005). Characterization and properties of metallic iron nanoparticles: spectroscopy, electrochemistry, and kinetics. *Environmental Science & Technology, 39*(5), 1221–1230.

Oturan, M. A., & Aaron, J. J. (2014). Advanced oxidation processes in water/wastewater treatment: Principles and applications. A review. *Critical Reviews in Environmental Science and Technology, 44*(23), 2577–2641.

Parra, S., Nadtotechenko, V., Albers, P., & Kiwi, J. (2004). Discoloration of azo-dyes at biocompatible pH-values through an Fe-histidine complex immobilized on Nafion via Fenton-like processes. *Journal of Physical Chemistry B, 108*, 4439–4448.

Pereira, M. C., Coelho, F. S., Nascentes, C. C., Fabris, J. D., Araújo, M. H., Sapag, K., Luiz, C. A. O., & Lago, R. M. (2010). Use of activated carbon as a reactive support to produce highly active-regenerable Fe-based reduction system for environmental remediation. *Chemosphere, 81*(1), 7–12.

Pérez, M. C. M., Martínez, S., de Lecea, C., & Linares, S. A. (1997). Platinum supported on activated carbon cloths as catalyst for nitrobenzene hydrogenation. *Applied Catalysis A: General, 151*(2), 461–475.

Pignatello, J. J., Oliveros, E., & MacKay, A. (2006). Advanced oxidation processes for organic contaminant destruction based on the Fenton reaction and related chemistry. *Critical Reviews in Environmental Science and Technology, 36*(1), 1–84.

Ramirez, J. H., Maldonado-Hódar, F. J., Pérez-Cadenas, A. F., Moreno-Castilla, C., Costa, C. A., & Madeira, L. M. (2007). Azo-dye Orange II degradation by heterogeneous Fenton like reaction using carbon-Fe catalysts. *Applied Catalysis B: Environmental, 75*(3-4), 312–323.

Romero, A., Santos, A., & Vicente, F. (2009). Chemical oxidation of 2, 4-dimethylphenol in soil by heterogeneous Fenton process. *Journal of Hazardous Materials, 162*(2-3), 785–790.

Segura, Y., Martínez, F., & Melero, J. A. (2013). Effective pharmaceutical wastewater degradation by Fenton oxidation with zero-valent iron. *Applied Catalysis B: Environmental, 136–137*, 64–69.

Shi, J. G., Ai, Z. H., & Zhang, L. Z. (2014). Fe@Fe_2O_3 core-shell nanowires enhanced Fenton oxidation by accelerating the Fe (III)/Fe (II) cycles. *Water Research, 59*, 145–153.

Singh, P., Raizada, P., Kumari, S., Kumar, A., Pathania, D., & Thakur, P. (2014). Solar-Fenton removal of malachite green with novel Fe^0-activated carbon nanocomposite. *Applied Catalysis A: Genenral, 476*, 9–18.

Su, Y. F., Cheng, Y. L., & Shih, Y. H. (2013). Removal of trichloroethylene by zerovalent iron/activated carbon derived from agricultural wastes. *Journal of Environmental Management, 129*, 361–366.

Subbaramaiah, P. V., Srivastava, V. C., & Mall, I. D. (2014). Catalytic oxidation of nitrobenzene by copper loaded activated carbon. *Separation and Purification Technology, 125*, 284–290.

Tan, D., Zeng, H. H., Liu, J., Yu, X. Z., Liang, Y. P., & Lu, L. J. (2013). Degradation kinetics and mechanism of trace nitrobenzene by granular activated carbon enhanced microwave/hydrogen peroxide system. *Journal of Environmental Science, 25*(7), 1492–1499.

Thankappan, R., Nguyen, T. V., Srinivasan, S. V., Vigneswaran, S., Kandasamy, J., & Loganathan, P. (2015). Removal of leather tanning agent syntan from aqueous solution using Fenton oxidation followed by GAC adsorption. *Journal of Industrial and Engineering Chemistry, 21*, 483–488.

Velo-Gala, I., Lopez-Penalver, J. J., Sanchez-Polo, M., & Rivera-Utrilla, J. (2014). Comparative study of oxidative degradation of sodium diatrizoate in aqueous solution by H_2O_2/Fe^{2+}, H_2O_2/Fe^{3+}, Fe (VI) and UV, H_2O_2/UV, $K_2S_2O_8$/UV. *Chemical Engineering Journal, 241*, 504–512.

Wang, W., Zhou, M., Mao, Q., Yue, J., & Wang, X. (2010). Novel NaY zeolite-supported nanoscale zero-valent iron as an efficient heterogeneous Fenton catalyst. *Catalysis Communications, 11*(11), 937–941.

Wang, A. J., Cheng, H. Y., Liang, B., Ren, N. Q., Cui, D., Lin, N., Kim, B. H., & Rabaey, K. (2011). Efficient reduction of nitrobenzene to aniline with a biocatalyzed cathode. *Environmental Science & Technology, 45*(23), 10186–10193.

Wang, L., Yao, Y. Y., Zhang, Z. H., Sun, L. J., Lu, W. Y., Chen, W. X., & Chen, H. X. (2014). Activated carbon fibers as an excellent partner of Fenton catalyst for dyes decolorization by combination of adsorption and oxidation. *Chemical Engineering Journal, 251*, 348–354.

Wu, J. H., Yin, W. Z., Gu, J. J., Li, P., Wang, X. D., & Yang, B. (2013a). A biotic Fe^0-H_2O system for nitrobenzene removal from groundwater. *Chemical Engineering Journal, 226*, 14–21.

Wu, L. M., Liao, L. B., Lv, G. C., Qin, F. X., He, Y. J., & Wang, X. Y. (2013b). Micro-electrolysis of Cr(VI) in the nanoscale zero-valent iron loaded activated carbon. *Journal of Hazardous Materials, 254–255*, 277–283.

Wu, S. C., Wen, G. D., Zhong, B. W., Zhang, B. S., Gu, X. M., Wang, N., & Su, D. S. (2014). Reduction of nitrobenzene catalyzed by carbon materials. *Chinese Journal of Catalysis, 35*(6), 914–921.

Xiao, J. N., Yue, Q. Y., Gao, B. Y., Sun, Y. Y., Kong, J. J., Gao, Y., Li, Q., & Wang, Y. (2014). Performance of activated carbon/nanoscale zero-valent iron for removal of trihalomethanes (THMs) at infinitesimal concentration in drinking water. *Chemical Engineering Journal, 23*, 63–72.

Yao, Y. Y., Wang, L., Sun, L. J., Zhu, S., Huang, Z. F., Mao, Y. J., Lu, W. Y., & Chen, W. X. (2013). Efficient removal of dyes using heterogeneous Fenton catalysts based on activated carbon fibers with enhanced activity. *Chemical Engineering Science, 101*, 424–431.

Zhang, H., Jin, Z., Han, L., & Qin, C. (2006). Synthesis of nanoscale zero valent iron supported on exfoliated graphite for removal of nitrate. *Transactions of Nonferrous Metals Society of China, 16*(1), 345–349.

Zhang, R. M., Li, J. S., Liu, C., Shen, J. Y., Sun, X. Y., Han, W. Q., & Wang, L. J. (2013a). Reduction of nitrobenzene using nanoscale zero-valent iron confined in channels of ordered mesoporous silica. *Colloids and Surfaces A: Physicochemical and Engineering Aspects, 425*, 108–114.

Zhang, Y. Y., Jiang, H., Zhang, Y., & Xie, J. F. (2013b). The dispersity-dependent interaction between montmorillonite supported nZVI and Cr(VI) in aqueous solution. *Chemical Engineering Journal, 229*, 412–419.

Zhang, Y. L., Zhang, K., Dai, C. M., & Zhou, X. F. (2014). Performance and mechanism of pyrite for nitrobenzene removal in aqueous solution. *Chemical Engineering Science, 111*, 135–141.

Zhou, H. M., Shen, Y. Y., Lv, P., Wang, J. J., & Fan, J. (2013). Degradation of 1-butyl-3-methylimidazolium chloride ionic liquid by ultrasound and zero-valent iron/activated carbon. *Separation and Purification Technology, 104*, 208–213.